# HOMOPOLYGALACTURONAN MOLECULAR SIZE IN PLANT CELL WALL MATRICES VIA PARAMAGNETIC ION AND NITROXYL AMIDE DIPOLAR SPIN–SPIN INTERACTIONS

PETER L. IRWIN,* MICHAEL D. SEVILLA,‡ AND WALEE CHAMULITRAT*
*U. S. Department of Agriculture, Eastern Regional Research Center, Philadelphia, Pennsylvania 19118; and ‡Department of Chemistry, Oakland University, Rochester, Michigan 48063

ABSTRACT $Mn^{2+}$, $Cu^{2+}$, and nitroxyl amines have been shown to bond to plant homopolygalacturonan matrices in a spatially sequential fashion. As a consequence of this special form of cooperativity the lattice constant ($\kappa$), determined from Van Vleck's second moment relationship, approaches 1 only when the average number of dipolar interactions per spin approaches 1 (e.g., an array of dimers). Assuming that one paramagnetic ion or nitroxyl amide pair is bonded per polymer block within the matrix when $\kappa = 1$, the anionic ligand's average degree of polymerization ($\overline{DP}$) can be estimated from the concentration of bonded paramagnetic dimers (e.g., $[1/\chi]_{\kappa\sim1} = \overline{DP}$; $\chi$ is the mole fraction of bonded paramagnetic dimers). We have utilized this technique to estimate the average molecular size of homopolygalacturonan blocks in intact higher plant cortical cell walls ($\overline{DP}$ ~83), *Nitella* cell walls ($\overline{DP}$ ~27) and a commercially available galacturonic acid polymer ($\overline{DP}$ ~35). The $\overline{DP}$ determined from both the intact cortical cell wall lattice and the polygalacturonan were similar to literature values; these findings argue that the electron paramagnetic resonance, (EPR) dipolar spin–spin interaction technique reported herein is a valid approach for estimating molecular size in plant cell walls.

## INTRODUCTION

The primary cell wall and middle lamellar complex of plants is roughly analogous to the skeleton of animals. These mostly polysaccharide matrices are biologically important because they are believed to influence cell morphology and structure as well as take part in the size exclusion and ion exchange properties of the symplast. Uronic acid-containing polysaccharides are one of the most abundant matrix components of the primary cell walls of most higher plants (1) and certain algae (2, 3). These sugar acid-containing matrix polysaccharides (1) exist as homopolymers with rhamnosyl residues, upon which neutral sugar side chains reside, interrupting the polyuronide main chain into regions or blocks. Heretofore, the structural features of uronic acid-containing cell wall components have been studied almost exclusively by the chemical analysis of fragments released from the matrix via acid or enzymatic hydrolysis (1–7) and therefore provide little information about the higher-order structure or molecular size of these sugar acid domains in intact cell wall systems. One of the major problems concerning the determination of molecular size of these important cell wall polymers is that they can form extended arrays in aqueous solution and, therefore, the determination of molecular weights by means of colligative or size exclusion properties can provide spurious information due to aggregational effects (6, 8, 9). Thus, any method which could provide a reasonable estimation of the average molecular size of these blocks in an intact lattice would be of potential use in further understanding the structure and function of the matrix polysaccharides.

Generally, dipolar interactions (10) are one of the most useful homogeneous interactions in electron paramagnetic resonance spectroscopy. These spin–spin interactions have long been utilized in molecular biology (11–15) to determine, for example, metal–metal distances between two binding sites on the surface of an enzyme (13). In previous studies (16–18) direct evidence was presented that certain paramagnetic species ($Mn^{2+}$, $Cu^{2+}$, or a nitroxyl amine) can ionically, as a metal complex, or covalently, as an amide, bond to plant homopolygalacturonans in a spatially sequential fashion. Thus, the occupation of some initial carboxyl site by a metal (16, 17) or by the reaction with the nitroxyl amine to form an amide (18) induces an alteration in the polymer's structure which allows for nearest neighbor site occupation. This process results in adjacent site bonding to form a sequential array. The evidence for this phenomenon was: (*a*) that the second moments ($\langle H^2 \rangle_{ave}$) or line widths ($\Delta H_{pp}$) of the electron paramagnetic reso-

Please address all correspondence to Dr. Irwin.

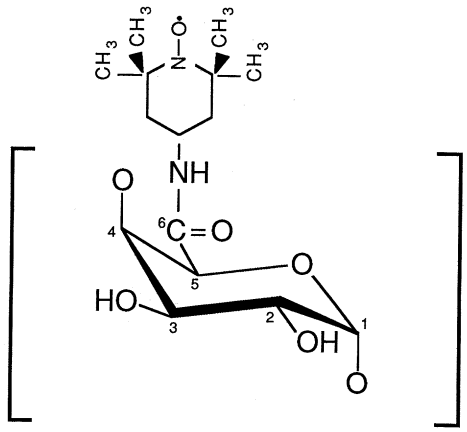


FIGURE 1 Chemical structure of the 4-amino-2,2,6,6-tetramethylpiperidine-1-oxyl-amide derivative of a galacturonan block segment.

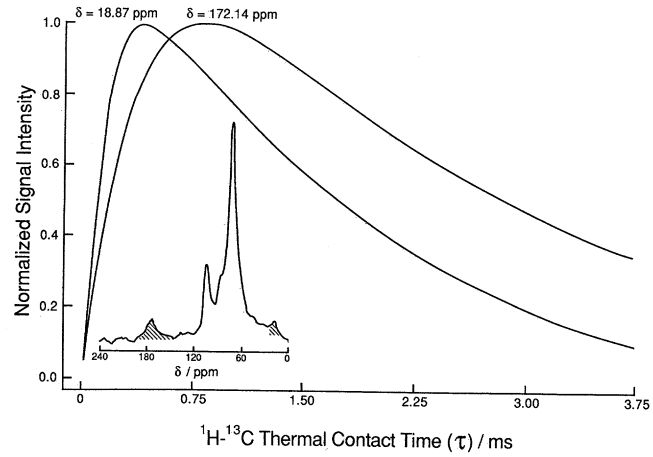


FIGURE 2 $^1$H-$^{13}$C polarization transfer experiment on *Nitella* cell walls showing the calculated best-fit curves (Eq. 2) for the remotely protonated C=O resonance, mainly due to the acid sugar matrix (2, 25), and a highly-protonated resonance, the $CH_3$ of rhamnose. Parameters yielding these curves were: $\gamma_{CH_3} = 1.04$ (the maximum measured signal intensities have been normalized to a maximum value of 1), $\alpha_{CH_3} = 144$ μs, $\beta_{CH_3} = 2.02$ ms, $\gamma_{CO} = 1.54$, $\alpha_{CO} = 354$ μs, $\beta_{CO} = 2.53$ ms. *Inset figure:* CPMAS NMR spectrum (0.8 ms of $^1$H-$^{13}$C thermal contact) obtained using 20,000 transients with a recycle time of ~2 s.

nance (EPR) spectrum of cell wall acid sugar polymer salts of $Cu^{2+}$ and $Mn^{2+}$ or the nitroxyl amide of a homopolygalacturonan were highly broadened at relatively low concentrations; (*b*) the broadening effect was reversible by competitive bonding with a diamagnetic species of similar size; (*c*) at the dilute limit, where the concentration of bonded paramagnetic species approached zero, the observed $\Delta H_{pp}$ or $\langle H^2 \rangle_{ave}$s approached those of the paramagnetic moiety in a dilute glass matrix. Here we present evidence that the concentration of the bonded paramagnetic species at which the number of dipolar interactions per spin is approximately one is related to the average degree of polymerization of the acid sugar ligand.

## MATERIALS AND METHODS

Preparation of the higher plant cortical cell wall matrices (16, 17) and the nitroxyl amides of polygalacturonic acid (18), the structure of which is shown in Fig. 1, were performed as described elsewhere. Mature cells of the giant fresh water alga, *Nitella,* were purchased from Carolina Biological Supply Co., Burlington, NC.[1] Fully-elongated (e.g., the third or fourth cell from the apex) internodal cells which were ≥2.5 cm and without apparent parasites were utilized for the $Cu^{2+}$ ion exchange experiments (19). The cells were excised from the main filament and plasmolysed in the presence of 1% (wt/vol) $Na^+$ dodecyl sulfate (Aldrich Chemical Co., Inc., Milwaukee, WI). The cytoplasmic components were easily removed by gently flattening the cells out in a direction parallel to the main axis. The *Nitella* cell wall material was then sonicated 10 s in a fresh medium as above followed by a second rinsing in deionized and distilled water. Only transparent cells were kept for experimental purposes. The wall material prepared in this fashion was partially dehydrated consecutively in 20 and 40% (vol/vol) ethanol:$H_2O$ at least 2 h each. $Cu^{2+}$ exchange experiments were performed by equilibrating wall matrix powders in $10^{-6}$–$10^{-2}$ M $CuCl_2$ in 40% (vol/vol) ethanol:H2O. After ~24 h, the solutions were decanted and the powdered cell wall ghosts were washed three times in 40% (vol/vol) ethanol:$H_2O$. The treated wall material was then fully dehydrated consecutively in 60, 80, and 100% (vol/vol) ethanol:$H_2O$ followed by critical point drying. This method of drying has been long observed by microscopists to maintain cell wall fiber morphology because the specimens are not subjected to either the surface tension forces or the freezing and sublimation boundaries associated with other drying procedures. Cross polarization and magic angle sample spinning $^{13}$C nuclear magnetic resonance (CPMAS NMR) spectra of *Nitella* cell wall material prepared in this fashion reveal no aliphatic resonances, other than rhamnose's C-6 and/or acetylated polysaccharide's (δ ~19 ppm) methyl resonances, indicating a low abundance of lipids from cytoplasmic membranal components which might have adhered to the wall matrix (Fig. 2, *insert*).

For EPR experiments, intact dehydrated and critical point dried cell wall matrices (3–5 mg dry weight) or the lyophilized nitroxyl amides of a homopolygalacturonan were loaded into 3 × 4 mm (inside diameter × outside diameter) quartz EPR tubes. All EPR spectra were collected on a E-109B spectrometer (Varian Associates, Inc., Palo Alto, CA) interfaced with the IBM 9000 computer system (IBM Instruments Inc., Danbury, CT). Quantitation of the various paramagnetic species and spectroscopic parameters for $Mn^{2+}$ and the nitroxyl amides have been described previously (16–18). $Cu^{2+}$ line widths were measured directly from the first derivative $g_\perp$ component as the difference in field strength, expressed in Gauss, between the maximum and minimum amplitude ($\Delta H_{pp}^{obs.}$) with a scan range of 1.6 kG, 3 kG field set, 4 G modulation amplitude, 9.1 GHz, and ~1.5 mW microwave frequency and power, respectively. This measure of line width is directly proportional to the true anisotropic line's width ($\Delta H_{pp}^{obs.} = \Delta H_{pp}^{calc.} \div 1.17$). Second moments ($\langle H^2 \rangle_{ave}$) for both $Mn^{2+}$ (Fig. 3) and nitroxyl (18) amide computer simulations and experimental spectra were calculated by the method of even moments (20)

$$\langle H^2 \rangle_{ave} = \frac{\Delta H}{\Delta H^2 \sum_{j=1}^{m} \sum_{i=1}^{j} \left\{ \frac{\delta I(H)}{\delta H} \right\}_i} \sum_{j=1}^{m} \sum_{i=1}^{j} (H_j - H_0)^2 \left\{ \frac{\delta I(H)}{\delta H} \right\}_i . \quad (1)$$

In Eq. 1, $\{\delta I(H)/\delta H\}_i$ represents the relative first derivative signal intensity of each data point, ΔH the magnetic field interval between adjacent data points (0.67 G) and $H_0$, the magnetic field value (at $g_{iso}$) where the double integral was ½ maximum. $Mn^{2+}$ $\langle H^2 \rangle_{ave}$ values (Fig. 3) varied linearly with respect to the empirical line broadening factor (LBF; Fig. 3, inset) which, as shown previously (16), varied linearly with the ratio of simulated Gaussian line widths ($\Delta H_{pp}$) to line separations in the experimental LBF range. Similar simulations have been performed for

[1]Reference to brand or firm name does not constitute endorsement by the U.S. Department of Agriculture over others of a similar nature not mentioned.

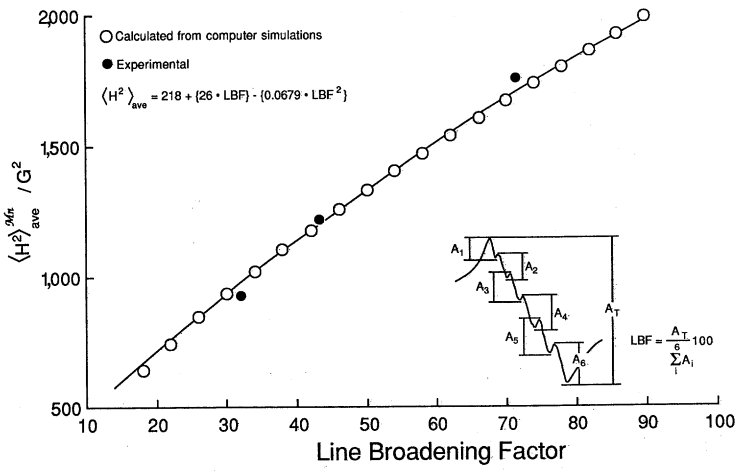


FIGURE 3 Relationship between the second moment ($\langle H^2 \rangle_{ave}$) of $Mn^{2+}$ derived by numerical integrations (Eq. 1) for experimental (*closed circles*) and computer-generated first derivative Gaussian lines (*open circles*) and the line broadening factor (LBF). The LBF is defined in the inset figure.

the nitroxyl amides of homopolygalacturonans (18) which indicate that the nitroxyl's $\langle H^2 \rangle_{ave}$s changed linearly with the empirical line broadening measure, $d_1/d$ (21), which is the amplitude between the low field first derivative maximum and the high field minimum divided by the total amplitude of the central hyperfine line. Thus, these findings all indicate that the LBF as well as $d_1/d$ measures of line broadening for cell wall bonded $Mn^{2+}$ and nitroxyl amides are directly proportional to their respective $\langle H^2 \rangle_{ave}$s.

CPMAS NMR spectra (8 kHz spectral width) were obtained at a $^{13}C$ frequency of 15 MHz on a FX-60QS spectrometer (JEOL USA, Analytical Instruments Div., Cranford, NJ) with a $^1H$ decoupling field strength of 11 G. 1,024 time domain data points were sampled and zero-filled to 4,096 points for fast Fourier transformation. All chemical shifts were assigned relative to hexamethylbenzene's (HMB) $CH_3$ resonance ($\delta$ = 17.6 ppm) based on the position of trimethylsilane. Approximately 200–300 mg of dehydrated and critical point dried cell wall matrices were spun ~2.5 kHz at the magic angle (54.7°) in a Kel-F bullet-type rotor (Kel Instruments Co., Inc., Clifton, NJ). Calibration of the magic angle was performed with HMB before each experiment. We have utilized CPMAS NMR for quantitative purposes because it is difficult to measure the concentration of the carboxylate functional groups, which are the bonding sites, in a solid lattice made up of mostly insoluble polysaccharides using normal chemical analyses (22). For quantitative analysis, resonance peak areas were measured by triangulating to the baseline and taking three measurements, gravimetrically or with a planimeter, per resonance. Spectra used to determine the molar composition of nonesterified carboxyl groups in the higher plant cell wall matrix (16, 22) were acquired using a 0.8 ms $^1H$-$^{13}C$ thermal contact time. These conditions have been shown (22) to provide reasonable quantitation of the higher plant cell wall acid sugar polymers as long as there is an absence of paramagnetic species which necessarily perturb the rotating frame spin–lattice relaxation process. Calculation of the molar concentration of binding sites in the *Nitella* cell wall matrices was somewhat problematic since the concentrations reported in the literature (~30% [wt/wt]; reference 23) were significantly different than those which we measured utilizing only one contact time (0.8 ms) as described previously (16, 17, 22). The relative signal responses (Fig. 2) for the C=O and $CH_3$ spin domains of $^1H$-$^{13}C$ polarization transfer clearly exemplify why it is sometimes problematic to measure the macroscopic magnetization of different spin populations having radically different degrees of protonation utilizing only a single cross polarization transfer time. The carbonyl resonance is particularly troublesome if the rotating frame spin-lattice relaxation rate ($\beta^{-1}$) is large relative to the rate of $^1H$ to $^{13}C$ magnetization transfer ($\alpha^{-1}$) due to its remote protonation. In the case of the *Nitella* cell wall sample this latter principle is particularly true since $\beta^{-1}_{C=O}$ is fast relative to $\alpha^{-1}_{C=O}$ and causes the observed maximum of C=O macroscopic magnetization, seen at ~800 $\mu$s, to be ~50% smaller than the true macroscopic magnetization ($\gamma$). Thus, quantitative analysis of *Nitella* CPMAS NMR spectra using only one contact time ($\tau$) could lead to underestimation of the carboxylate functionality since the rate of polarization transfer was slow relative to the directly-protonated spin species, such as the carbohydrate ring carbons or methyl groups. Since a good estimation of available binding sites is critical to the calculation of molecular size, we have performed a detailed cross polarization analysis on both the higher plant cell wall system, published elsewhere (22), and the *Nitella* system (Fig. 2). Fig. 2 presents a typical $^{13}C$ cross polarization experiment on *Nitella* cell wall matrices with best fit (24) curves utilizing the Gauss-Newton iteration procedure for both remotely-protonated resonances (C=O; $\delta$ = 172.14 ppm), which are predominantly due to the carboxyl group of the sugar acid matrix polymers (2, 25), and highly-protonated resonances (the $CH_3$ of rhamnose and acetylated sugars; $\delta$ = 18.87 ppm). For the CPMAS NMR analysis Eq. 2 describes the scalar value of the macroscopic magnetization vector ($\Phi$) which varies as a function of $^1H$ to $^{13}C$ thermal contact time ($\tau$).

$$\Phi[\tau; \alpha, \beta, \gamma] = \gamma \cdot \{1 - e^{-\tau/\alpha} + e^{-\tau/\beta}\} - \gamma. \qquad (2)$$

In this relation $\gamma$ is the theoretical maximum signal intensity of the particular resonance in question, $\alpha$ is the reciprocal $^1H$-$^{13}C$ polarization transfer rate, $\beta$ is the rotating frame spin-lattice relaxation time. Having a good estimate of $\gamma$ is important in the calculation of the number of binding sites, on a mole/gram cell wall basis, because $\gamma$ is equivalent to what the equilibrium macroscopic $^{13}C$ magnetization scalar value would be at an infinite value of $\tau$ without rotating-frame spin-lattice relaxation. Upon performing the complete $^1H$-$^{13}C$ thermal contact time experiment, using the model described above and solving for $\gamma$ with respect to the C=O, $CH_3$ as well as nonspecific ring carbon resonances, the calculated percentages of acid sugar-containing polymers and $CH_3$-containing polysaccharides in the *Nitella* cell wall sample were found to be 35 and 4%, respectively.

## RESULTS AND DISCUSSION

When a system of electron spins, $\mathbf{S}_i$, interacts with an applied magnetic field vector, $\mathbf{H}$, to produce a resonance line each magnetic moment precesses about the $z$ component of $\mathbf{H}$ with a frequency equal to $-g\beta H_z(\mathbf{H} = \mathbf{H}_{applied} + \mathbf{H}_{local})$. The scalar value as well as orientation of $\mathbf{H}$ will vary from one point dipole to the next when there is a high spin density, which results in a significant $H_{z,\,local}$ field contribution, and causes a spreading out of the observed precessional frequencies resulting in line broadening (26). However, each resonance line has a width determined by the sum of the dipolar and exchange spin–spin interactions in accordance with the complete

Hamiltonian operator ($\mathcal{H}$). The $\mathcal{H}$ operator system (27) for an ensemble of interacting spins consists of a set of $i$th terms, the separate Hamiltonians for each spin species (Zeeman energy), as well as a set of $i$th-$j$th terms which are the sum of the various interaction operators (20, 26, 27–34)

$$\mathcal{H} = g\beta H_z \sum_i S_{z,i} + \sum_{i>j} \tilde{\mathcal{A}}_{ij} \mathbf{S}_i \cdot \mathbf{S}_j + \mathcal{H}_{\text{dipolar}} \quad (3)$$

$$\mathcal{H}_{\text{dipolar}} = g^2\beta^2 \sum_{i>j} \left\{ \frac{\mathbf{S}_i \cdot \mathbf{S}_j}{r_{ij}^3} - 3\,\frac{[\mathbf{r}_{ij} \cdot \mathbf{S}_i][\mathbf{r}_{ij} \cdot \mathbf{S}_j]}{r_{ij}^5} \right\}. \quad (4)$$

In these relations, $g$, $\beta$, and $S$ have their usual meaning; $\mathbf{r}$ is the distance vector between the $i$th and $j$th spins and $\tilde{\mathcal{A}}_{ij}$ is a term which is proportional to the exchange integral ($\mathcal{J}$). The summation subscript, $i > j$, identifies that each pair of interactions should be counted only once. Of course, exact computation of the Hamiltonian interaction profile is not feasible (27). One of the most practical alternative techniques (10, 26, 35, 36) for evaluating the dipolar contribution to spin–spin coupling, first developed by Van Vleck (29), is the so-called method of moments. The second moment ($\langle H^2 \rangle_{\text{ave}}$), which is related (29) to a Gaussian's line width ($\Delta H_{\text{pp}} = 2\langle H^2 \rangle_{\text{ave}}^{1/2}$), is defined as (27, 29)

$$\langle H^2 \rangle_{\text{ave}} = \int_{-\infty}^{\infty} (H - H_0)^2 f(H)\, dH \Big/ \int_{-\infty}^{\infty} f(H)\, dH, \quad (5)$$

whereupon $H_0$ is the position coordinate for the exact center of the EPR spectrum. All the data presented here assume that the interaction profile is completely dipolar in nature with very little contribution of spin (27, 28, 30, 33, 37, 38) or coulomb (39) exchange, another form of homogeneous (32) spin–spin interaction. Spin or coulomb exchange interactions can cause a narrowing in the EPR spectrum due to the rapid fluctuation, $\sim\mathcal{J}/h$, and averaging (27) of $\mathbf{H}_{\text{local}}$ due to mutual spin flips. We have disregarded any exchange effects since homopolygalacturonan intrachain carboxylate distances, which constitute the bonding loci, are relatively large (≅10–15 Å; 16–18, 40).

Fig. 4 presents the calculated $\langle H^2 \rangle_{\text{ave}}$s for $Mn^{2+}$ bound to a higher plant cortical cell wall matrix as a function of

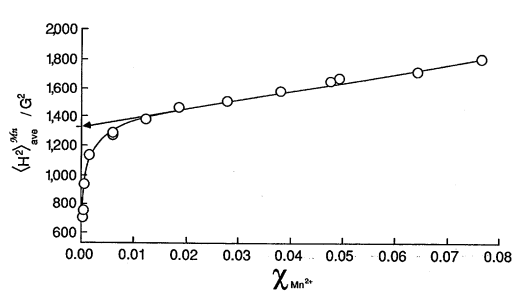


FIGURE 4 Dependency of higher plant cell wall-bound $Mn^{2+}$ second moments ($\langle H^2 \rangle_{\text{ave}}$) on the molar ratio of $Mn^{2+}$ dimers to the total anionic ligand monomers ($\chi$). The arrow points to that value of $\langle H^2 \rangle_{\text{ave}}$ taken to be where $\kappa = 1$ (Eqs. 6 and 7).

$\chi_{Mn^{2+}}$, the total moles of the bound dimer (e.g., total moles of $Mn^{2+}$ bound ÷ 2) divided by the total moles of uronic acid monomer. If one considers calculations for a randomly-oriented lattice (16, 17, 29) the following relationships are true

$$\langle H^2 \rangle_{\text{ave}} = \frac{3}{5} g^4\beta^4 h^{-2} S(S+1) \sum_{i>j} \frac{1}{r_{ij}^6} \quad (6)$$

$$\sum_{i>j} \frac{1}{r_{ij}^6} = \left\{ \frac{\kappa^2}{d^6} \right\}. \quad (7)$$

Thus, assuming that only dipolar spin–spin interactions occur, for reasons discussed previously, the second moment is related to the reciprocal sixth power of the distance between a group of $i$-$j$th interacting spins (10, 20, 26, 27, 31, 33, 34, 36, 41). In the above equations $d$ is the nearest neighbor distance parameter for an ordered array and $\kappa$ varies with the lattice arrangement (17). We have utilized the $\kappa$ term because changes in $\langle H^2 \rangle_{\text{ave}}$ cannot be attributed entirely to the nearest neighbor distance parameter. As a paramagnetic species begins to fill the lattice an increase in the number of dipolar spin–spin interactions will occur at each $i$th spin. For example, $\kappa = 1$ for two interacting spins, 1.4 for a linear array, 2.45 for a two-dimensional hexagonal array with six nearest neighbors (Fig. 5) and $\kappa = 3.46$ for a three-dimensional hexagonal close packing array with

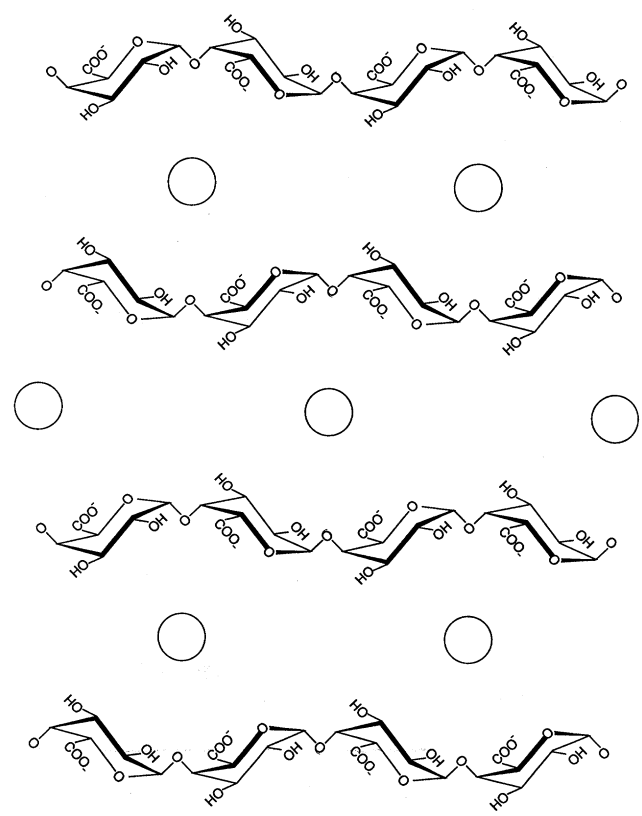

FIGURE 5 Two-dimensional hexagonal array (17) with six nearest neighbors ($\kappa = 2.45$; open circles represent the divalent cations), relative to the center ion, of a homopolygalacturonan lattice.

12 nearest neighbors. Considering nearest neighbor interactions only, $\kappa^2$ is an estimate of the number of near neighbor interactions at distance $d$ even in a system with an extended array due to the decreased weighting of distant interactions. As $\kappa$ approaches 1, $\kappa^2$ provides an accurate estimation of the number of near neighbor interactions per point dipole (42) since, in this low concentration region, the number of distant interactions are negligible. As shown before (17), we can approximate the dimer-only nearest neighbor distance parameter from the extrapolated zero concentration-$\langle H^2 \rangle_{ave}$ intercept (Fig. 4); at this value of $\langle H^2 \rangle_{ave}$ (e.g., at the arrow), $\kappa$ is ~1. Assuming that $d$ remains relatively constant with addition of the paramagnetic species, we can calculate the number of strongly interacting spins per $i$th point dipole using the expressions above (Eqs. 8 and 9) from each of the empirically-derived values of $\langle H^2 \rangle_{ave}$. If the sequential bonding mechanism (16–18) is true, the concentration of bound paramagnetic species at which the number of dipolar spin–spin interactions is ~1 is related to the size of the homopolygalacturonan blocks since the probability of bonding at near neighbor sites is far more likely than any other position within that same block. Because of this type of bonding we can assume, as a first approximation, that one paramagnetic ion pair bonds per polymer block within the matrix when $\kappa$ is ~1. If this assumption is true the anionic ligand's average degree of polymerization ($\overline{DP}$) within each block copolymer can be estimated from $\chi$ when $\kappa = 1$

$$\{1/\chi\}_{\kappa\sim 1} = \overline{DP}, \tag{8}$$

whereupon $\chi$ is the mole fraction of paramagnetic dimers bound.

Fig. 6 presents the higher plant cell wall matrix $\kappa^2$ values as a function of $\chi^{-1}$ for both $Cu^{2+}$ and $Mn^{2+}$. We have presented two $\chi^{-1}$ axis systems representing different models for the localization of the methyl ester domains (ME). In Model 1 we assume that the ME functional groups of homopolygalacturonans are equally represented within each block; in Model 2 we assume, as has been proposed previously (1), that MEs are confined to their own separate blocks or domains and therefore do not reside in the same regions as the free acid form. The $\overline{DP}$ estimated for Models 1 and 2 were ~83 and 37, respectively.

The major evidence that the hydrophobic ME functionalities occur sequentially, as opposed to a random distribution throughout the lattice, is that the enzyme which de-esterifies these functional groups does so sequentially (1, 4) or blockwise. Other evidence for this hypothesis is that (17), as the anionic ligand matrix fills with a paramagnetic divalent cation, the number of strong dipolar spin–spin interactions is larger than one would expect for a random array of MEs which would necessarily disrupt the paramagnetic lattice with diamagnetic holes. That the ME groups occur sequentially does not prove, however, that these domains reside in separate blocks. Indeed, in this system, if a paramagnetic amine is specifically reacted (18) to the cell wall matrix acid sugar polymers (Fig. 7 *A*) to form the nitroxyl amide the ME resonance disappears (Fig. 7 *B*); this apparent broadening effect is completely reversible by reduction of the nitroxyl (N-O·) to the hydroxyl amide (N-OH) with ascorbate. This apparent loss of the ME resonance could be due to several mechanisms (43–45): the paramagnetic's effect on (*a*) rotating-frame spin-lattice relaxation (the spectra shown were collected with 0.8 ms of $^1H$ to $^{13}C$ thermal contact), (*b*) the spectral density of the ME resonance or (*c*) $T_1$-driven $T_2$

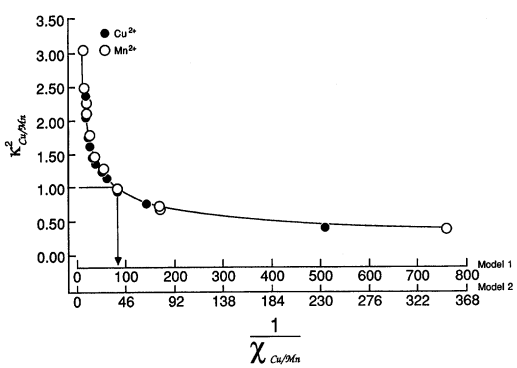


FIGURE 6 Plot of $\kappa^2$ for $Cu^{2+}$ (*solid circles*) and $Mn^{2+}$ (*open circles*) bound to the higher plant cell wall lattice versus reciprocal $\chi$ for two models of the methyl ester (ME) domains. Model 1 assumes that the ME domains are equally distributed in blocks along with the free acid form ($\chi$ = moles dimer/total moles uronide). Model 2 assumes that the free acid domain does not coexist with the ME domain ($\chi$ = moles dimer/moles uronic acid monomer). The arrows point to that region on the curve where $\{1/\chi\}_{\kappa\sim 1} \simeq \overline{DP}$ of the homopolygalacturonan blocks for the two models ($\overline{DP}$ = 83 or 37 for models 1 or 2, respectively). Typically broadened $Cu^{2+}$ spectra have been shown previously (22).

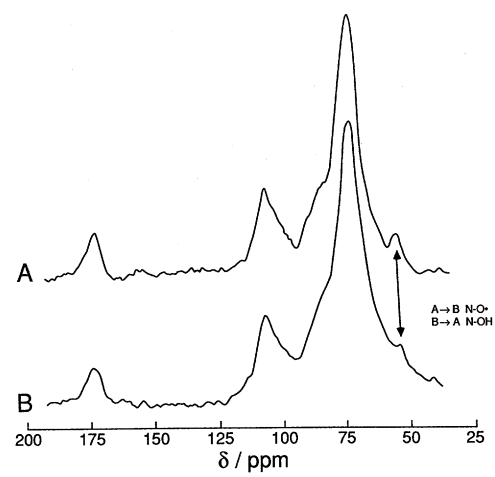


FIGURE 7 CPMAS NMR spectra of higher plant cell wall matrices (0.8 ms of $^1H$-$^{13}C$ thermal contact) obtained using 10,000 transients (*A*) or 40,000 transients (*B*) with recycle time of ~2 s. Spectrum *A* represents the control experiment (no nitroxyl amide). Spectrum *B* is the same as *A* but with the free acid reacted (18) with 4-amino-2,2,6,6-tetramethylpiperidine-1-oxyl to form the amide (~2 × $10^{19}$ spins/g). Upon reduction of the nitroxyl group with ascorbate *B* reverts to *A*.

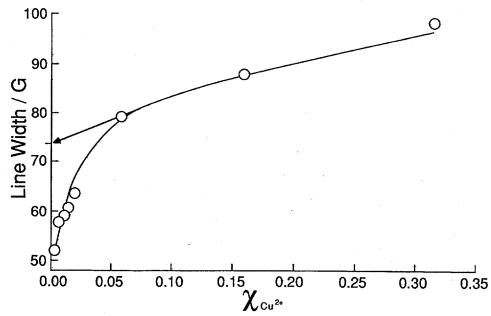


FIGURE 8 Dependency of *Nitella* cell wall-bound $Cu^{2+}$ line widths ($\Delta H_{pp}$) on the molar ratio of $Cu^{2+}$ dimers to the total anionic ligand monomers ($\chi$). The arrow points to that value of $\Delta H_{pp}$ taken to be where $\kappa = 1$ (Eqs. 6 and 7; $\Delta H_{pp} \simeq 2\langle H^2\rangle_{ave}^{1/2}$). Typically broadened $Cu^{2+}$ spectra have been shown previously (22).

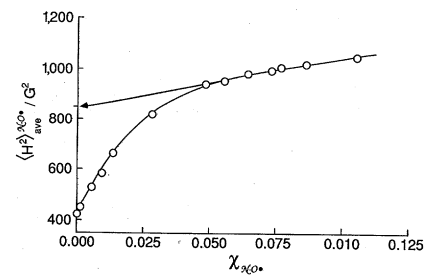


FIGURE 10 Dependency of polygalacturonate-bonded 4-amino-2,2,6,6-tetra-methylpiperidine-1-oxyl (as the amide; reference 18) second moments ($\langle H^2\rangle_{ave}$) on the molar ratio of spin-label dimers to the total anionic ligand monomers ($\chi$). The arrow points to that value of $\langle H^2\rangle_{ave}$ taken to be where $\kappa = 1$ (Eqs. 6 and 7).

whereupon that part of the free induction decay associated with the ME resonance is not sampled due to a rapid decay of its FID envelope in the dead time before data acquisition. Regardless of the mechanism these data support the hypothesis that the ME functional groups occur, at least in part, as proposed in Model 1 since electron-nuclear dipolar spin–spin interactions occur only with relatively near neighbor species. Model 1 is also supported by the fact that the larger homopolygalacturonan fragments released from a higher plant cell wall matrix, after partial enzymatic hydrolysis (5), had a $\overline{DP}$ of ~70 which is reasonably close to the $\overline{DP}$ calculated via the dipolar spin–spin interaction technique described above.

*Nitella* is an important plant taxa with respect to cell wall chemistry because it is frequently used as a model system for higher plant species (19) in studies of cell wall elongation. The major difference in primary structure between the higher plant and the *Nitella* systems is that this alga has very few ME functional groups (23) as shown in the CPMAS NMR spectrum (Fig. 2, *inset*) whereupon this particular resonance ($\delta \sim 54$ ppm) is barely observable. EPR experiments on $Cu^{2+}$-labeled *Nitella* cell walls (Figs. 8 and 9) utilizing the method described above indicate that this species of large fresh water algae had smaller block homopolygalacturonans, $\{1/\chi\}_{\kappa\sim1} \sim 27$, than the higher plant matrix discussed above. Relating our estimated block homopolygalacturonan $\overline{DP}$ to the previous models of ME localization is not meaningful since this plant species has so few hydrophobic domains. If the block size of the acidic polysaccharide lattice is related to $\chi^{-1}$, as we suggest, the dipolar spin–spin interaction technique could be useful in studying the involvement of matrix polysaccharides in cell extensive growth.

If $\chi$ is related to the average size of homopolygalacturonan blocks when $\kappa$ is ~1, as we have proposed, then experiments with a similar system of known molecular size should provide a reasonable test. In the experiments shown in Figs. 10 and 11 the nitroxyl amine, 4-amino-2,2,6,6-tetramethylpiperidine-1-oxyl, which has been shown (18) to bond covalently to plant homopolygalacturonans in a way remarkably similar to divalent paramagnetic species, was reacted to various levels with a matrix of known $\overline{DP}$. Again, we assume that the extrapolated zero concentration-$\langle H^2\rangle_{ave}$ intercept (Fig. 10) is equal to $\langle H^2\rangle_{ave}$ when $\kappa$ is ~1. Plotting $\kappa^2$ as a function of $\chi^{-1}$ (Fig. 11) illustrates that, utilizing the dipolar spin–spin interaction method, the measured $\overline{DP}$ of this homogeneous polymer was ~35. The number average molecular weight for these same polymers (6) from reducing end-group titration has been demonstrated to be 6,100 ± 400 D or having a $\overline{DP} \simeq 30$ and is in

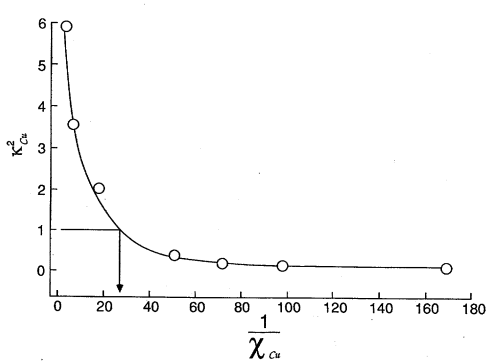


FIGURE 9 Plot of $\kappa^2$ for $Cu^{2+}$ bound to the *Nitella* cell wall lattice versus reciprocal $\chi$. The arrows point to that region on the curve where $\{1/\chi\}_{\kappa\sim1} \simeq \overline{DP}$ of the homopolygalacturonan blocks ($\overline{DP} = 27$).

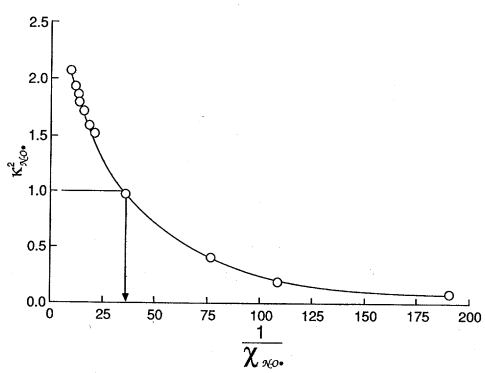


FIGURE 11 Plot of $\kappa^2$ for a polygalacturonate-bonded 4-amino-2,2,6,6-tetra-methylpiperidine-1-oxyl lattice versus reciprocal $\chi$. The arrows point to that region on the curve where $\{1/\chi\}_{\kappa\sim1} \simeq \overline{DP}$ of the homopolygalacturonan blocks ($\overline{DP} = 35$).

good agreement with the EPR dipolar spin–spin interaction method.

## CONCLUSION

In this manuscript we have argued that the concentration of the bonded paramagnetic species where the number of dipolar interactions per spin is ~1 is related to the average degree of polymerization of acid sugar matrix polysaccharides in a higher plant as well as an algal cell wall system. Using the assumptions stated previously we have calculated that the average molecular size of the acidic matrix polysaccharide blocks in higher plant cell walls was on the order of 83; literature values of $\overline{DP}$ vary from ≅25 (4) to ≅70 (5) for enzymatically-cleaved fragments and strongly argue that our technique provides reasonable values. Using these same assumptions for a polymer of known molecular size we calculated a $\overline{DP}$ of ≅35 which was in good agreement with the true number average molecular weight as measured by reducing end-group titration (6). Since the $\overline{DP}$ determined from both the intact cortical cell wall system and the polygalacturonan were similar to literature values, our findings argue that the EPR dipolar spin–spin interaction method reported herein can be a useful nondestructive technique for establishing the degree of polymerization in these systems. If the assumptions stated previously are true, our EPR method indicated that *Nitella* cell walls had a $\overline{DP}$ ≅ 27 which was significantly smaller than the block homopolygalacturonans in the higher plant matrix discussed above. This observation suggests that there are fundamental structural differences between the matrix polysaccharides in the *Characeae* and those in vascular plants.

*Received for publication 21 September 1987 and in final form 13 April 1988.*

## REFERENCES


1. Jarvis, M. C. 1984. Structure and properties of pectin gels in plant cell walls. *Plant Cell Environ.* 7:153–164.
2. Anderson, D. M. W., and N. J. King. 1961. Polysaccharides of the Characeae. II. The carbohydrate content of *Nitella translucens. Biochim. Biophys. Acta.* 52:441–449.
3. Anderson, D. M. W., and N. J. King. 1961. Polysaccharides of the Characeae. III. The carbohydrate content of *Chara australis. Biochim. Biophys. Acta.* 52:449–454.
4. Powell, D. A., E. R. Morris, M. J. Gidley, and D. A. Rees. 1982. Conformations and interactions of pectins. II. Influence of residue sequence on chain association in calcium pectate gels. *J. Mol. Biol.* 155:517–531.
5. Konno, H., Y. Yamasaki, and K. Katoh. 1986. Enzymatic degradation of pectic substances and cell walls purified from carrot cultures. *Phytochemistry (Oxf.).* 25:623–627.
6. Fishman, M. L., P. E. Pfeffer, R. A. Barford, and L. W. Doner. 1984. Studies of pectin solution properties by high performance size exclusion chromatography. *J. Agric. Food Chem.* 32:372–378.
7. Knee, M. 1978. Properties of polygalacturonate and cell cohesion in apple fruit cortical tissue. *Phytochemistry (Oxf.).* 17:1257–1260.
8. O'Beirne, D., and J. P. Van Buren. 1983. Size distribution of high weight species in pectin fractions from Idared apples. *J. Food Sci.* 48:276–277.
9. Davis, M. A. F., M. J. Gidley, E. R. Morris, D. A. Powell, and D. A. Rees. 1980. Intermolecular association in pectin solutions. *Int. J. Biol. Macromol.* 2:330–332.
10. Smith, T. D., and J. R. Pilbrow. 1974. The determination of structural properties of dimeric transition metal ion complexes from EPR spectra. *Coord. Chem. Rev.* 13:173–278.
11. Cohn, M., and J. Reuben. 1971. Paramagnetic probes in magnetic resonance studies of phosphoryl transfer enzymes. *Acc. Chem. Res.* 4:214–222.
12. Niccolai, N., E. Tiezzi, and G. Valensin. 1982. Manganese (II) as a magnetic relaxation probe in the study of biomechanisms and of biomacromolecules. *Chem. Rev.* 82:359–384.
13. Balakrishnan, M. S., and J. J. Villafranca. 1978. Distance determinations between metal ion sites of *Escherichia coli* glutamine synthetase by electron paramagnetic resonance using Cr(III)-nucleotides as paramagnetic substrate analogues. *Biochemistry.* 17:3531–3538.
14. Taylor, J. S., J. S. Leigh, and M. Cohn. 1969. Magnetic resonance studies of spin-labeled creatine kinase system and interaction of two paramagnetic probes. *Proc. Natl. Acad. Sci. USA.* 64:219–226.
15. Reed, G. H., and M. Cohn. 1970. Electron paramagnetic resonance spectra of manganese(II)-protein complexes: manganese(II)-concanavalin A. *J. Biol. Chem.* 245:662–667.
16. Irwin, P. L., M. D. Sevilla, and J. J. Shieh. 1984. ESR evidence for sequential divalent cation binding in higher plant cell walls. *Biochim. Biophys. Acta.* 805:186–190.
17. Irwin, P. L., M. D. Sevilla, and C. L. Stoudt. 1985. ESR spectroscopic evidence for hydration- and temperature-dependent spatial perturbations of a higher plant cell wall paramagnetic ion lattice. *Biochim. Biophys. Acta.* 842:76–83.
18. Irwin, P. L., M. D. Sevilla, and S. F. Osman. 1987. Spectroscopic evidence for spatially sequential amide bond formation in plant homopolygalacturonans. *Macromoles.* 20:1222–1227.
19. Van Cutsem, P., and C. Gillet. 1983. Proton-metal cation exchange in the cell wall of *Nitella flexilis. Plant Physiol. (Bethesda).* 73:865–867.
20. Poole, C. P., Jr. 1983. Origin of the moments of spectral lines. *In* Electron Spin Resonance: A Comprehensive Treatise on Experimental Techniques. John Wiley & Sons, Inc., New York. 459–576.
21. Likhtenshtein, G. I. 1974. Double Paramagnetic Labels. *In* Spin Labeling Methods in Molecular Biology, English translation. John Wiley & Sons, Inc., New York. 37–65.
22. Irwin, P. L., W. V. Gerasimowicz, P. E. Pfeffer, and M. Fishman. 1985. $^{1}H$-$^{13}C$ polarization transfer studies of uronic acid polymer systems. *J. Agric. Food Chem.* 33:1197–1201.
23. Morikawa, H., and M. Senda. 1974. Nature of the bonds holding pectic substances in *Nitella* cell walls. *Agric. Biol. Chem.* 38:1955–1960.
24. Draper, N., and H. Smith. 1981. Introduction to nonlinear estimation. *In* Applied Regression Analysis. John Wiley & Sons Inc., New York. 458–529.
25. Morikawa, H., K. Tanizawa, and M. Senda. 1974. Infrared spectra of *Nitella* cell walls and orientation of carboxylate ions in the wall. *Agric. Biol. Chem.* 38:343–348.
26. Pryce, M. H. L., and K. W. H. Stevens. 1950. The theory of magnetic resonance-line widths in crystals. *Proc. Phys. Soc. (Lond.)* A63:36–51.
27. Abragam, A., and B. Bleaney. 1970. Introduction to electron paramagnetic resonance. *In* Electron Paramagnetic Resonance of Transition Ions. Oxford University Press, Oxford. 1–94.
28. Anderson, P. W., and P. R. Weiss. 1953. Exchange narrowing in paramagnetic resonance. *Rev. Mod. Phys.* 25:269–276.
29. Van Vleck, J. H. 1948. The dipolar broadening of magnetic resonance lines in crystals. *Physiol. Rev.* 74:1168–1183.
30. Judeikis, H. S. 1964. Errors in the evaluation of moments of a paramagnetic resonance line. *J. Appl. Physiol.* 35:2615–2617.
31. Shia, L., and G. Kokoszka. 1974. EPR of $Mn_xMg_{1-x}(HCOO)_2 \cdot$

$2H_2O$: a two-dimensional magnetic lattice. *J. Chem. Phys.* 60:1101–1105.

32. McMillan, J. A. 1968. Experimental Methods. *In* Electron Paramagnetism. Reinhold Book Corp., New York. 131–151.
33. Gorter, C. J., and J. H. Van Vleck. 1947. The role of exchange interaction in paramagnetic absorption. *Phys. Rev.* 72:1128–1129.
34. Leigh, J. S., Jr. 1970. ESR rigid-lattice line shape in a system of two interacting spins. *J. Chem. Phys.* 52:2608–2612.
35. Eaton, S. S., K. M. More, B. M. Sawant, and G. R. Eaton. 1983. Use of the EPR half-field transition to determine the interspin distance and the orientation of the interspin vector in systems with two unpaired electrons. *J. Am. Chem. Soc.* 105:6560–6567.
36. Grant, W. J. C., and M. W. P. Strandberg. 1964. Statistical theory of spin–spin interactions in solids. *Physiol. Rev.* 135:A715–A726.
37. Gulley, J. E., D. Hone, D. J. Scalapino, and B. G. Silbernagel. 1970. Exchange narrowing: magnetic resonance line shapes and spin correlations in paramagnetic $KMnF_3$, $RbMnF_3$, and $MnF_2$. *Physiol. Rev.* 1:1020–1030.
38. Carroll, J. C. G., S. M. McMurry, J. Corish, and B. Henderson. 1985. Exchange interactions between $Cr^{3+}$ ions in magnesium oxide. II. Electron spin resonance spectra. *J. Phys. C.: Solid State Phys.* 18:6409–6418.
39. Humphries, G. M. K., and H. M. McConnell. 1982. Nitroxide spin labels. *Meth. Exp. Phys.* 20:53–122.
40. Morvan, C., M. Demarty, and M. Thellier. 1979. Titration of isolated cell walls of *Lemna minor,* L. *Plant Physiol. (Bethesda).* 63:1117–1122.
41. Hyde, J. S., and K. V. S. Rao. 1978. Dipolar-induced electron spin-lattice relaxation in unordered solids. *J. Magn. Res.* 29:509–516.
42. Shinar, J., and V. Jaccarino. 1982. On the rigid lattice dipolar broadening of the $Mn^{2+}$ EPR in the dilute limit. *Phys. Lett.* 91A:132–134.
43. Gerasimowicz, W. V., K. B. Hicks, and P. E. Pfeffer. 1984. Evidence for the existence of associated lignin-carbohydrate polymers as revealed by carbon-13 CP-MAS solid-state NMR spectroscopy. *Macromoles.* 17:2597–2603.
44. Eaton, D. R., and W. D. Phillips. 1965. Nuclear magnetic resonance of paramagnetic molecules. *Adv. Magn. Res.* 1:103–148.
45. Redfield, A. G. 1965. The theory of relaxation processes. *Adv. Magn. Res.* 1:1–32.